Persistence of skin-resident memory T cells within an epidermal niche

Ali Zaid[a,1], Laura K. Mackay[a,1], Azad Rahimpour[a], Asolina Braun[a], Marc Veldhoen[b], Francis R. Carbone[a], Jonathan H. Manton[c], William R. Heath[a,2], and Scott N. Mueller[a,2,3]

[a]Department of Microbiology and Immunology, Peter Doherty Institute for Infection and Immunity, The University of Melbourne, Parkville, VIC 3010, Australia; [b]Laboratory for Lymphocyte Signalling and Development, The Babraham Institute, Cambridge CB22 3AT, United Kingdom; and [c]Department of Electrical and Electronic Engineering, The University of Melbourne, Parkville, VIC 3010, Australia

Edited by Rafi Ahmed, Emory University, Atlanta, GA, and approved February 26, 2014 (received for review December 2, 2013)

Barrier tissues such as the skin contain various populations of immune cells that contribute to protection from infections. These include recently identified tissue-resident memory T cells (T_{RM}). In the skin, these memory $CD8^+$ T cells reside in the epidermis after being recruited to this site by infection or inflammation. In this study, we demonstrate prolonged persistence of epidermal T_{RM} preferentially at the site of prior infection despite sustained migration. Computational simulation of T_{RM} migration within the skin over long periods revealed that the slow rate of random migration effectively constrains these memory cells within the region of skin in which they form. Notably, formation of T_{RM} involved a concomitant local reduction in dendritic epidermal γδ T-cell numbers in the epidermis, indicating that these populations persist in mutual exclusion and may compete for local survival signals. Accordingly, we show that expression of the aryl hydrocarbon receptor, a transcription factor important for dendritic epidermal γδ T-cell maintenance in skin, also contributes to the persistence of skin T_{RM}. Together, these data suggest that skin tissue-resident memory T cells persist within a tightly regulated epidermal T-cell niche.

intravital imaging HSV-1 infection | Langerhans cells | Brownian motion

The skin is a complex organ that acts as a primary barrier between the body and the environment. Multiple leukocyte subsets reside within the main compartments of the skin, the dermis and the epidermis, as well as the hair follicles that are contiguous with the epidermis. Populations of macrophages, dendritic cells, mast cells, γδ T cells and αβ T cells are present in the dermis, and Langerhans cells (LCs) and dendritic epidermal γδ T cells (DETCs) lie in a strategic network in the epidermis (1). We recently described a population of memory $CD8^+$ T cells that enter the epidermis and hair follicles during infection or inflammation and become long-lived populations of tissue-resident memory T cells (T_{RM}) (2–5). These memory T cells are sequestered in this site and are distinct from circulating effector memory (T_{EM}) and central memory (T_{CM}) populations (3, 6). Memory $CD8^+$ T cells in the epidermis display a dendritic morphology and move at a slower velocity than T cells within the dermis. These memory T cells are sequestered in the skin epithelial layer and do not recirculate to other tissues. In contrast, memory $CD4^+$ T cells are found within the dermis and at least a proportion of these cells are capable of recirculating around the body (3, 7).

In this study, we sought to further examine the mechanisms of T_{RM} persistence within the skin. We reveal that skin T_{RM} persist at the site of their formation and despite displaying a sustained mode of random migration, the slow rate of this movement locally constrains these memory cells. Examination of other cells in this environment showed that although epidermal T_{RM} regularly interact with LC, these interactions were not required for persistence. In contrast, skin tissue-resident memory T cells replaced DETCs in the epidermis, seeming to compete for space within the epidermal niche. We found that expression of the aryl hydrocarbon receptor (AhR) is required for long-term persistence of T_{RM}, indicating that this may be a common survival pathway for T cells residing in the epidermis.

Results

Migration of Epidermal T_{RM}. To understand how T_{RM} persist in the skin and contribute to local protective immunity we sought to characterize the behavior of these memory T cells within their natural environment. We used a well-established model of cutaneous HSV infection (8) and MHC class I-restricted T-cell receptor (TCR) transgenic mice specific for an immunodominant glycoprotein B epitope ($gB_{498–505}$) (9). $CD8^+$ T cells from these gBT-I mice expressing EGFP were transferred into recipient C57BL/6 (B6) mice to track virus-specific T cells following HSV infection using intravital two-photon microscopy of the skin. As we and others have observed previously (3, 10), memory $CD8^+$ T cells were present in the epidermis and displayed a unique dendritic morphology (Fig. 1*A*). These T_{RM} were highly dynamic, demonstrating active probing of their environment with dendrites that rapidly extended and retracted (Movie S1). In many cases, multibranched dendrites formed, and cells could be observed extending cellular projections in multiple directions simultaneously.

Closer examination of the location of these skin T_{RM} revealed a highly constricted localization to the basal epidermis (Fig. 1*B*), immediately adjacent to and in contact with the basement membrane that separates the dermis from the epidermis (Fig. 1*C*). Identification of cells in each compartment was achieved using second harmonic generation (SHG) fluorescence to differentiate the collagen-rich dermis from the epidermis. This location defined the movement of the memory T cells, which extended dendritic projections laterally yet were not observed to probe

Significance

Tissue-resident memory T cells (T_{RM}) form in the skin where they are retained and can protect against subsequent infection. Using a combination of intravital imaging and mathematical modeling of skin T_{RM} that form after cutaneous herpes simplex virus 1 infection, we reveal that these memory T cells persist at the site of infection for the life of a mouse owing to slow random migration. We also report that T_{RM} compete with dendritic epidermal γδ T cells in skin for local survival signals, suggesting that T cells compete for space within an epidermal niche.

Author contributions: F.R.C., W.R.H., and S.N.M. designed research; A.Z., L.K.M., A.R., A.B., J.H.M., and S.N.M. performed research; M.V. contributed new reagents/analytic tools; A.Z., L.K.M., J.H.M., and S.N.M. analyzed data; and S.N.M. wrote the paper.

The authors declare no conflict of interest.

This article is a PNAS Direct Submission.

[1]A.Z. and L.K.M. contributed equally to this work.

[2]W.R.H. and S.N.M. contributed equally to this work.

[3]To whom correspondence should be addressed. E-mail: smue@unimelb.edu.au.

This article contains supporting information online at www.pnas.org/lookup/suppl/doi:10.1073/pnas.1322292111/-/DCSupplemental.

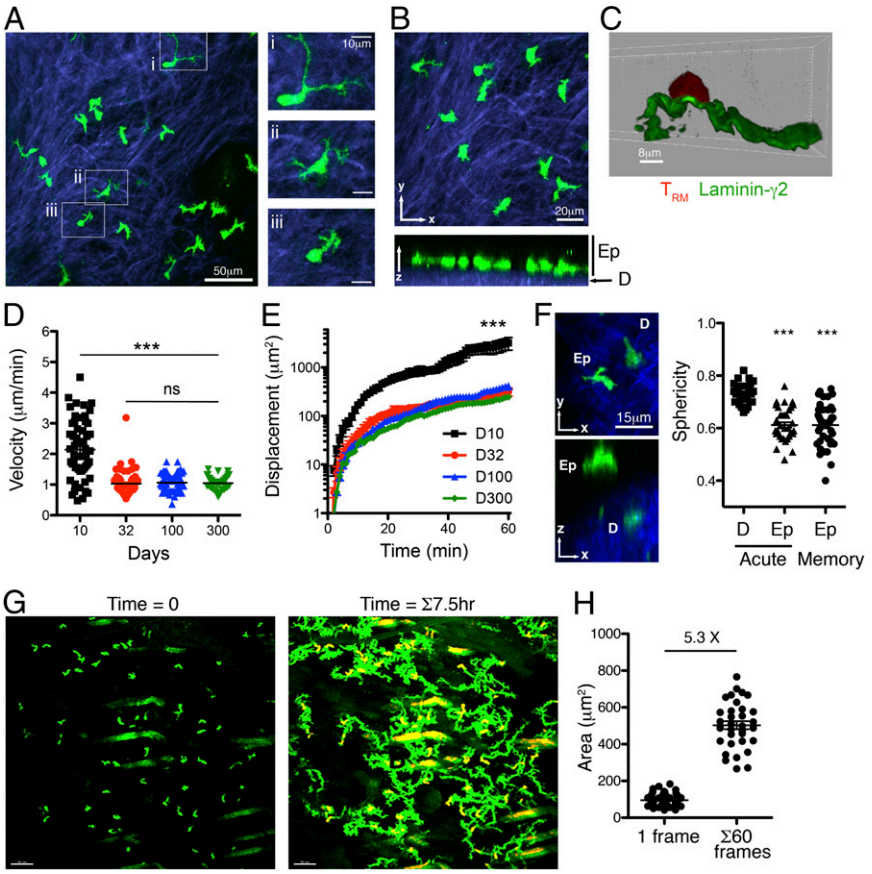

Fig. 1. Migration of skin T_{RM} at the site of prior infection. (*A*) gBT-I.GFP $CD8^+$ T cells (green) imaged by two-photon microscopy in the skin 32 d after HSV infection. Examples of different cell morphologies are magnified in i–iii. SHG (blue) delineates the collagen-rich dermis. Images correspond to Movie S1. (*B*) T_{RM} are located within the basal epidermis (Ep), adjacent to the SHG^+ dermis (D). (*C*) T_{RM} contact the basement membrane at the dermis–epidermal border. Tissue sections of skin containing gBT-I.DsRed $CD8^+$ T cells were costained with anti-laminin-γ2 antibodies. (*D*) Mean velocity and (*E*) displacement of T_{RM} migrating within the epidermis at the indicated times after HSV infection. ***$P < 0.0001$; ns, not significant. (*F*) Epidermal location defines the dendritic morphology of skin T_{RM}. Shown is a representative example of an epidermal and a dermal gBT-I T-cell 10 d after HSV infection. Sphericity measurements of dermal and epidermal gBT-I T cells 10 d (acute) and 32 d (memory) after HSV infection are plotted. (*G*) Time-lapse imaging of gBT-I T_{RM} migration in the skin. (*Left*) The first frame of the movie; (*Right*) superimposed images taken at 3-min intervals over a 7.5-h period. Images correspond to Movie S4. (*H*) The average 2D surface area of individual T_{RM} was calculated from 10 individual images per cell collected over a 60-min period. The total surface area covered per cell was calculated from superimposed images taken each minute for 1 h. The fold difference between the average surface area at time 0 and 60 is shown.

upward toward the apical epidermis and stratum corneum, nor downward toward the dermis (Movie S2). This is in contrast to skin DETCs, whose dendrites probe the apical epidermis in the steady state (11). T_{RM} could also be observed within hair follicle epithelial layers, as well as entering and exiting hair follicles via the contiguous epidermis (Movie S3).

To further examine the behavior of the skin T_{RM}, we determined the migration velocity within the epidermis over time. T cells in the epidermis migrate considerably more slowly than T cells within the dermis and have a dendritic as opposed to amoeboid morphology (3), which is likely influenced by the dense cellularity of the epidermal layer as well as the signals T cells encounter in this environment. Notably, we found that epidermal $CD8^+$ T cells migrated faster and covered greater distances during the effector phase when the skin was inflamed (Fig. 1 *D* and *E*). The shape and behavior of skin T_{RM} suggested that the dendritic morphology was defined by their localization within the epidermis. We took advantage of the ability to distinguish dermal and epidermal T cells using SHG signals and used Imaris software to render the 3D surface of the T_{RM} and examined the shape of the cells by determining their relative sphericity. Notably, the sphericity of both effector (day 10) and memory (day 32) T cells present within the epidermis was identical (Fig. 1*F*). In contrast, $CD8^+$ T cells migrating within the dermis displayed more amoeboid cell morphology. These data show that epidermal T-cell morphology was dictated largely by the microanatomical location of the cells rather than a unique property of memory T cells.

The migration by virus-specific $CD8^+$ T cells in the epidermis reduced to a steady rate within 1 mo of infection and remained unchanged for at least 300 d. Although they only displayed a slow rate of migration, time-lapse imaging revealed that epidermal T_{RM} navigated a substantial proportion of the epidermal tissue in a matter of hours (Fig. 1*G* and Movie S4). We calculated the 2D surface area covered by T_{RM}, given that they move within a roughly 2D environment. By examining cells over time, we estimated that the memory T cells scan an area approximately five times the size of an average cell per hour (in this experiment, 60 frames) (Fig. 1*H*). This suggests a substantial ability of T_{RM} to survey their immediate environment over time (10), particularly given the restricted dimensions of this compartment and the observation that skin T_{RM} remain resident in the epidermis and do not recirculate through other tissues (3).

Persistence of Epidermal T_{RM} at the Site of Infection. We noted that the density of T_{RM} within the skin was greatest at the site of prior infection (lesion). Given that T_{RM} are motile, we wanted to determine whether these memory cells gradually diffused across the flank as they randomly patrol the epidermis. Numbers of T_{RM} at the lesion site were quantitated soon after infection and up to 1 y later by microscopy (Fig. 2*A*) or by flow cytometry by enumerating $CD103^+$ gBT-I T cells (Fig. 2*B*). Consistent with the preferential presence of T_{RM} within flank skin originally infected by HSV-1 (4), T_{RM} remained concentrated at the lesion site with no discernible change in their distribution over time. This suggested that these memory cells were largely constrained to the site of infection where they initially developed.

To determine whether such local persistence of T_{RM} could be explained by the slow migration of these cells, or alternately whether these cells were actively constrained to this site by local signals, we performed computational modeling to simulate the movement of T_{RM} populations for time periods considerably longer than we could image (months to years). Simulation of random cell migration was performed using measurements of T_{RM} velocity and displacement acquired in vivo over a period of 2–3 h. Modeling cell migration based on these parameters revealed that

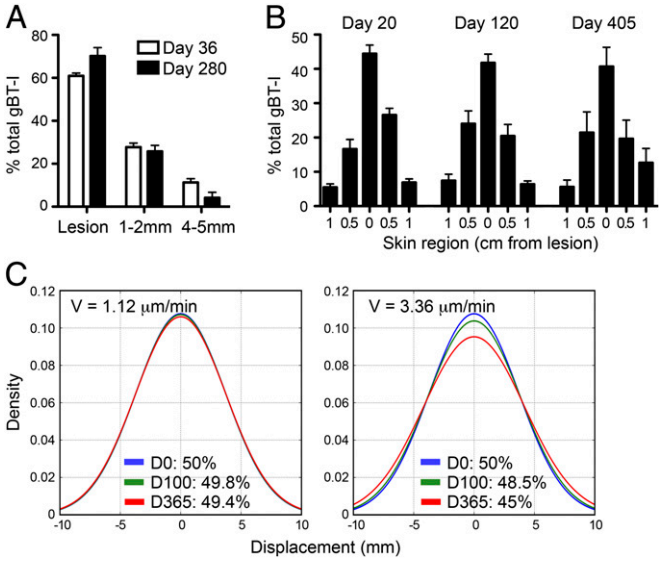

Fig. 2. Persistence of skin T_{RM} at the site of prior infection. (*A*) gBT-I CD8$^+$ T cells were quantitated at the lesion scar and two defined distances either side of the lesion by two-photon microscopy of skin 36 and 280 d after HSV infection. Data were averaged from four to six images per region from six mice. (*B*) Mice were analyzed 20, 120, or 405 d after HSV infection. Strips of flank skin 0.5 cm wide by 2 cm long at the site of infection (lesion) and on either side were harvested for enumeration of CD103$^+$ gBT-I CD8$^+$ T cells. Error bars represent SEM, n = 4–8 mice pooled from two independent experiments. (*C*) Computational modeling of T_{RM} migration. Movement of populations of cells distributed normally across the skin was simulated for 100 and 365 d based on an average cell velocity (V) of 1.12 μm/min (*Left*) or 3.36 μm/min (*Right*). The simulated region consisted of a 5-mm strip centered at 0. The frequency of cells within the simulated region was 50% at the beginning of the simulation (day 0) and the number of cells remaining within this region after the indicated time periods is shown.

the random location of the cells over extended periods (days) was equivalent to the random location of cells moving by Brownian motion, a consequence of the central limit theorem. The distribution of T_{RM} around the lesion could be approximated by a Gaussian distribution, which allowed us to model a population of T_{RM} where 50% of the cells were initially distributed across a 5-mm-wide strip of skin, similar to that observed in vivo and enumerated in Fig. 2*B*. Simulation of cell movement over periods of 100 and 365 d demonstrated only minimal change (from 50% to 49.8% and 49.4%, respectively) in the proportion of cells remaining within this region (Fig. 2*C*). Even if we tripled the average velocity of our model population to 3.3 μm/min, well above the observed velocity, the majority of T_{RM} still remained associated with the lesion after 1 y (from 50% to 45%). Thus, this model predicts relatively little diffusion of the cells across the skin by random movement within the lifespan of a mouse. These data indicate that the combination of slow and random migration by T_{RM} in the epidermis functions to constrain these memory cells largely to the region of skin in which they were formed, without the need for any physical or chemical barrier.

Skin T_{RM} Interact with LCs. The above observations suggested that active constraint of T_{RM} by extrinsic signals was not required for the cells to remain within the region of their formation. However, it does not rule out a role for signals that influence the speed of T_{RM} migration or competition for local survival signals. A dense meshwork of LCs is present within the epidermis between keratinocytes, where they capture environmental antigens and migrate to draining lymph nodes. LCs can stimulate T-cell responses, although their role in immunity and tolerance is poorly resolved (12). We wanted to determine whether T_{RM} interact regularly with LCs as they migrate through the epidermis. We used Langerin-GFP (Lg-GFP) mice that were transferred with gBT-I.DsRed CD8$^+$ T cells before HSV infection. During the memory phase, T_{RM} were observed to interact regularly with LCs, crawling over the numerous LC dendrites and interacting directly with LC cell bodies (Fig. 3 *A* and *B* and Movie S5). Quantification of T_{RM}–LC interactions revealed that half of the epidermal memory T cells were in contact with LC at all times during a 1-h imaging period (Fig. 3*C*) and only a very minor fraction of T_{RM} were not in contact with LCs at all in the same period. In contrast, LCs were sessile (mean velocity, 0.3 μm/min) and were positioned in a regularly spaced network, the density of which was not influenced by the presence or absence of T_{RM} (Fig. 3*D*). Thus, T_{RM} interact frequently with LCs as they migrate throughout the epidermis.

To reveal whether such T_{RM}–LC interactions were important for the migration or survival of memory T cells in the epidermis, we used mice expressing the diphtheria toxin (DT) receptor under control of the Langerin promoter (Lg-DTR) to selectively deplete LCs upon DT treatment. We transferred gBT-I.DsRed CD8$^+$ T cells into Lg-DTR or Lg-GFP mice before HSV infection. Upon establishment of memory, mice were treated with DT for 2 wk to deplete LCs. Ablation of the LC population for this period did not affect gBT-I numbers in the skin or spleen (Fig. 3*E*), and expression of surface molecules required for T_{RM} persistence, CD103 and CD69, was unchanged on cells in the skin (Fig. S1). The T_{RM} retained their dendritic morphology (Fig. 3*F*) yet displayed reduced migrational velocity (Fig. 3*G*). These data indicate that interactions with LCs are not required for T_{RM} persistence within this time period yet influence T_{RM} migration within the epidermis.

T_{RM} Persist Within an Epidermal Niche. Tightly interspersed with the epidermal LC network in mice is a similarly dense network of DETCs (13). These T cells are important for efficient wound

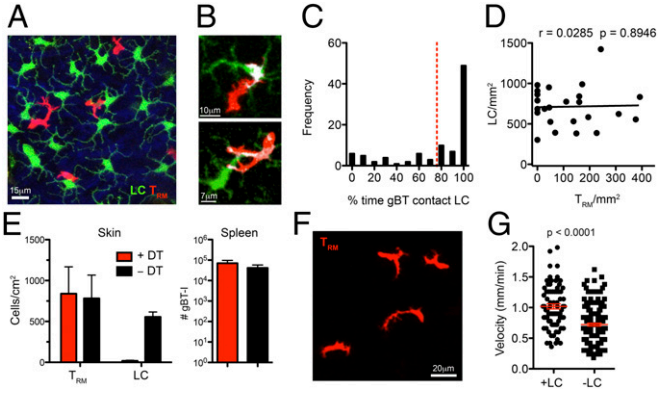

Fig. 3. T_{RM} interact with LC in the epidermis. (*A*–*C*) Skin T_{RM} interact frequently with LCs. (*A*) Representative image of gBT-I CD8$^+$ T cells (red) migrating among LCs in Lg-GFP mice in the epidermis of HSV-immune mice. (*B*) Interaction between a T_{RM} and LC in the skin at memory. Contact is represented by colocalization between the green and red channels (white). (*C*) Quantitation of the frequency of contacts between T_{RM} and LCs. Images were acquired at 1-min intervals for 45–60 min. (*D*) No correlation between T_{RM} and LC numbers in the skin after infection. Linear regression line and Pearson's correlation coefficient (r) are shown. (*E*–*G*) Ablation of LCs for 2 wk influences T_{RM} migration but not persistence. (*E*) Numbers of gBT-I CD8$^+$ T cells in the skin and spleen and LCs in the skin of Lg-DTR mice following 2 wk of treatment with DT. n = 6–8 mice per group. (*F*) Example of T_{RM} in Lg-DTR mice following 2 wk of treatment with DT. (*G*) Mean velocity of gBT-I CD8$^+$ T cells in Lg-GFP or Lg-DTR mice after DT treatment. Error bars represent SEM, n = 4–7 mice per group, from two to three independent experiments.

repair and respond to signals from stimulated keratinocytes (14, 15). Similarly, populations of epidermal T cells are also present in humans and may also contribute to wound repair (16). To identify skin DETCs we used CXCR6$^{GFP/+}$ knock-in mice (17). We transferred naïve gBT-I T cells into these mice followed by epicutaneous infection with HSV. Analysis of the skin by two-photon microscopy revealed that DETC are largely sessile and display a more pronounced dendritic morphology than T_{RM}, consisting of long stable dendrites (Fig. 4*A* and Movie S6). In comparison with LCs, fewer contacts between T_{RM} and DETCs were observed (Fig. 4*B*), although T_{RM} were capable of navigating through space occupied by DETCs by squeezing underneath the body of these cells (Fig. 4*C*). Of note, we also visualized endogenous T_{RM} in the skin of the CXCR6$^{GFP/+}$ mice that displayed the same morphology and mode of slow locomotion as gBT-I T cells (Movie S6). These endogenous T_{RM} were observed migrating within gaps in the DETC network. Moreover, extensive observation of DETCs and T_{RM} within the same and distinct areas of skin gave the impression of a consistent combined density.

To address the issue of T_{RM} and DETC density more specifically, we assessed the distribution of T_{RM} and DETCs by two-photon microscopy 1 mo after infection in CXCR6$^{GFP/+}$ mice. At the lesion site T_{RM} were present at a high density, which decreased with increasing distance from the lesion (Fig. 4*D*). Notably, we observed an inverse relationship between T_{RM} and DETCs, with DETCs largely absent from the lesion site (Fig. 4*E*). This suggested that DETCs were displaced at the site of infection and replaced by T_{RM}. The relationship between T_{RM} and DETC density in the epidermis was established with a Pearson's correlation coefficient (r = –0.76; Fig. 4*F*), demonstrating that as T_{RM} density increased there was a concomitant decrease in DETC numbers.

These data suggested that there is a mutual exclusion between T_{RM} and DETCs, possibly resulting from competition for a niche within the epidermis. We next examined the relationship between these two epidermal T-cell subsets in the absence of infection by intradermally injecting effector gBT-I T cells into B6 mice. The injected CD8$^+$ T cells can enter the epidermis and form long-lived T_{RM} in the absence of antigen (18). These T_{RM} seemed morphologically identical to cells that form after infection and migrated at a similar velocity (Movie S7). We observed regions with low numbers of T_{RM} and corresponding high numbers of DETCs and regions with high numbers of T_{RM} and low numbers of DETCs (Fig. 5*A*). Total numbers of T cells in each region were similar (Fig. 5*B*) and not higher than total numbers of T cells found in the epidermis of control mice (Fig. 5*C*), indicating that the T_{RM} did not add substantially to the epidermal T-cell pool, but rather replaced the DETCs resident in this site. This was supported by a significant negative correlation between T_{RM} and DETC numbers after intradermal injection (Fig. 5*D*). Control mice given PBS injections did not show a reduction in DETC numbers (Fig. S2), further suggesting that the transferred T cells displaced DETCs in this site.

We recently described several factors involved in regulating the formation and long-term survival of T_{RM} in the skin, including IL-15 and TGF-β (18). DETCs also require IL-15 for their development or survival (19), although they persist in the skin independently of TGF-β signals (20). Because T_{EM} and T_{CM} also require IL-15 for long-term maintenance (21), we considered whether other factors may specifically coregulate DETC and T_{RM} populations. DETCs express the AhR, a transcription factor required for their survival but not development (22, 23). We found that skin T_{RM} also express high levels of AhR in comparison with both naïve and memory T cells from the spleen (Fig. 5*E*). To examine a role for AhR in regulating T_{RM} populations in the skin, effector CD8$^+$ T cells from WT B6 and AhR$^{-/-}$ mice were injected in equal proportions into B6 mice treated on the flank 3 d earlier with the irritant 1-Fluoro-2,4-dinitrobenzene (DNFB). This model results in the formation of long-lived T_{RM} in the skin at the site of DNFB application (2). Both WT and AhR$^{-/-}$ CD8$^+$ T cells entered the skin in similar numbers, but over time AhR$^{-/-}$ T_{RM} disappeared from the skin, but not the spleen (Fig. 5*F*). Similar results were obtained with AhR$^{-/-}$ T_{RM} generated after intradermal injection (Fig. S3). Thus, we show that AhR facilitates T_{RM} persistence in the epidermis. Together, these data suggest that AhR ligands contribute to an epidermal T-cell niche, with antigen-experienced CD8$^+$ T cells effectively competing with DETCs for the same niche.

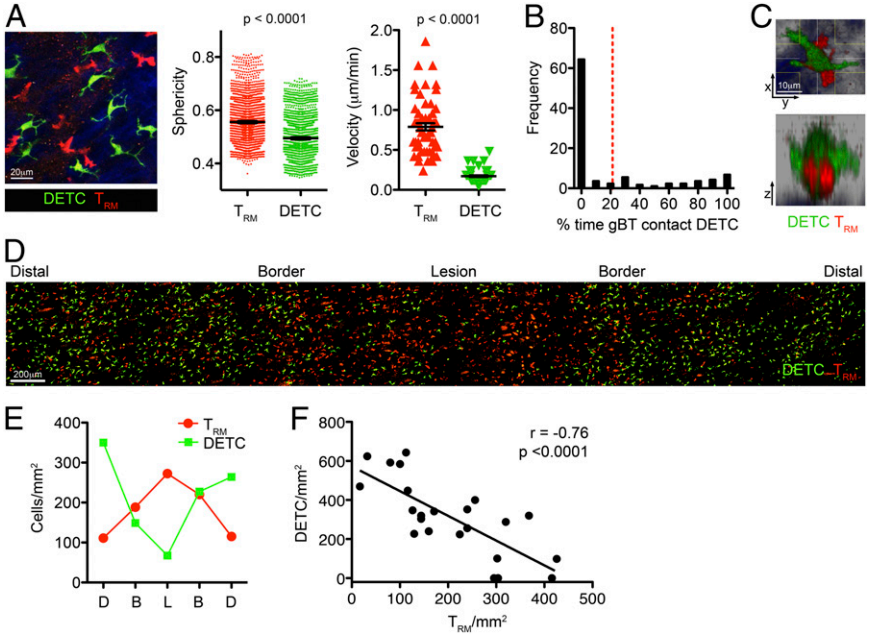

Fig. 4. T_{RM} displace DETCs at the site of infection. (*A*) Two-photon microscopy of T_{RM} and DETCs in the skin 30 d after HSV infection. A representative maximum intensity projection at the border of the lesion is shown. The sphericity and mean velocity of gBT-I.DsRed T_{RM} and CXCR6$^{GFP/+}$ DETC is shown. n = 6 mice. (*B*) Quantitation of the frequency of contacts between T_{RM} and DETCs. Images were acquired at 1-min intervals for 45–60 min. Data are compiled from 158 T_{RM} imaged from four mice. (*C*) T_{RM} migrating in the epidermis can travel beneath DETCs. A maximum intensity projection across x, y, and z dimensions is shown. (*D* and *E*) T_{RM} displace DETCs in the skin after infection. (*D*) Image of T_{RM} and DETCs in CXCR6$^{GFP/+}$ mice 30 d after HSV infection. (*E*) Quantitation of the density of cells within the indicated regions (B, border; D, distal region; and L, lesion) from the image in D. (*F*) Inverse correlation between T_{RM} and DETC numbers in the skin after infection. Linear regression line and Pearson's correlation coefficient (r) are shown. n = 7 mice.

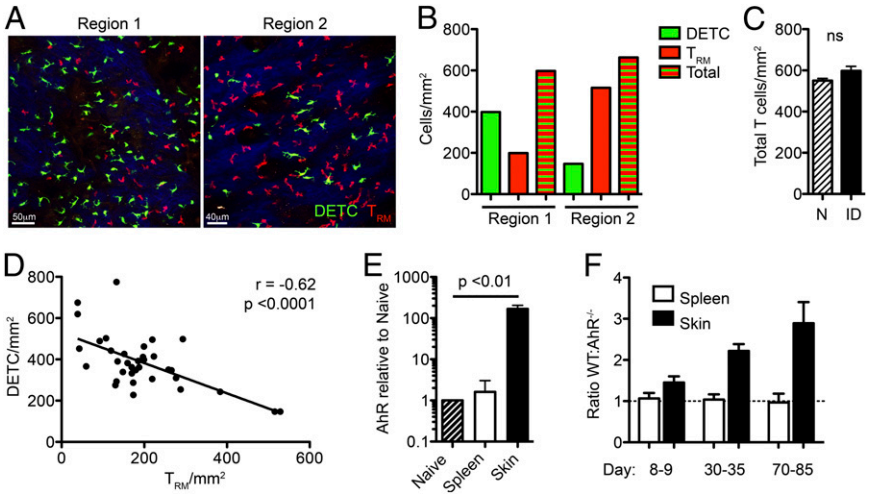

Fig. 5. T_{RM} persist within an epidermal niche. (*A*) T_{RM} form after intradermal injection and displace DETCs. Two representative examples of skin 30 d after injection of gBT-I effector T cells, showing a site with low numbers of T_{RM} (region 1) and a second with high numbers (region 2). (*B*) Enumeration of T_{RM} and DETCs in the images in *A*. (*C*) Enumeration of T_{RM} and DETCs in the skin of naïve mice (N) and 30 d after intradermal injection of gBT-I T cells (ID). ns, not significant. (*D*) Negative correlation between T_{RM} and DETC numbers in the skin after intradermal injection. Linear regression line and Pearson's correlation coefficient (r) are shown. $n = 6$ mice. (*E*) Expression of AhR in memory T-cell subsets 30 d after HSV infection quantitated by RT-PCR. $n = 3$–4. (*F*) Ratio of WT to $AhR^{-/-}$ $CD8^+$ T cells in the skin or spleen at the indicated times after i.v. transfer into mice treated with DNFB on the flank. Error bars represent SEM. Data pooled from two to three experiments with three to five mice per group.

Discussion

Recent studies have revealed that populations of tissue-resident memory $CD8^+$ T cells can form in a number of different tissues around the body, where they may provide the first lines of defense against reinfection (5, 24). For T_{RM} in tissues such as the skin, we are just beginning to understand their formation, which requires signals such as IL-15 and TGF-β and involves the progressive development of KLRG-1^{lo} effector cells into permanently resident cells that express high levels of the integrin CD103 and CD69 (18). Despite this, we still know relatively little about the behavior and functions of T_{RM} and the mechanisms of their long-term persistence.

Epidermal T_{RM} display a pronounced dendritic morphology (3, 10). We show here that these memory T cells are located at the dermal–epidermal border in contact with the basement membrane. T_{RM} were observed migrating underneath DETCs, suggesting a particular preference for contact with the basement membrane, which may provide traction for migration. As a part of this migration program, T_{RM} regularly contact the other immune cells in their environment: LCs, DETCs, and keratinocytes. Our data reveal regular contacts between T_{RM} and LCs as the T cells navigate through the uniform network of epidermal LCs. Depletion of LCs for 2 wk did not influence the morphology or survival of skin T_{RM}, yet migration was reduced, suggesting that LCs may provide locomotory signals to T_{RM}.

Persistence within the epidermis is a key characteristic of the skin T_{RM}, and we show that these cells are largely constrained to the region in which they form. Thus, despite their ability to migrate through the epidermis, skin T_{RM} remained concentrated at the site of prior infection rather than distributed over the skin of the flank. By modeling the migration of T_{RM} over longer periods we find that the slow mode of random migration effectively constrains these memory T cells to the local region in which they were formed. Moreover, we show an inverse relationship between skin T_{RM} and DETCs that is indicative of competition for persistence within an epidermal niche. It seems that DETCs either leave or die following HSV infection, the latter potentially the result of direct infection by this cytopathic virus (25). T_{RM} populate this DETC-replete skin, as well as the epidermis that borders the site of infection where many DETCs remain. Given that these populations of T cells likely need to compete for limited resources or space within the epidermis to survive, this may favor the persistence of T_{RM} in regions of skin where local DETC numbers are lower, and there is less competition. It is also possible that T_{RM} compete more effectively for space in the epidermis, providing an advantage that prevents repopulation of the skin by DETCs.

Our modeling data indicate that the slow and random movement of T_{RM} would maintain a large proportion of these cells within the region in which they formed, suggesting that additional competition for niche is likely to only further limit cells from straying beyond the lesion boundaries. We do not rule out the possibility that T_{RM} migration is influenced by other T cells in their environment; however, we found that T_{RM} motility was the same when cells were imaged where DETCs were absent (lesion) versus regions containing substantial numbers of DETCs (at the borders of lesions; Fig. S2). Interestingly, we reveal that following the intradermal injection of effector T cells, the formation of T_{RM} results in the displacement of a proportional number of DETCs. This raises the intriguing question of how T_{RM} that are induced by a subsequent infection in the same region of skin compete for space and whether newer T_{RM} can displace existing cells. Such information will be important if vaccines are designed that enhance the lodgment of T_{RM} within tissues. Additionally, it will be important to examine T_{RM} migration within human skin, where the epidermal layer is considerably thicker than in mice (26). If human skin T_{RM} migrate at a similar slow rate, with random direction in the steady state, and additionally have a larger area of tissue to navigate, we would predict that these memory cells would similarly persist in close proximity to the site of their formation.

Finally, we examined the role of AhR, a potential signal that may regulate the numbers of both αβ and γδ T cells within the epidermis and show that AhR contributes to the long-term persistence of T_{RM}. Recent studies have shown that expression of AhR is required for the homeostasis of several T-cell populations including γδ T cells resident in both the skin epidermis and gut epithelia and $CD8\alpha\alpha^+$ αβT cells in the gut (22, 23). Although natural ligands for AhR in the skin are less clear, dietary sources are critical for maintaining intestinal intraepithelial T cells. Our finding that epidermal T_{RM} also use AhR for maintenance, combined with data showing that T_{RM} can displace DETCs in the skin, suggest that epidermal T cells compete for space within a niche that is influenced at least in part by the availability of AhR ligands. Further work will be needed to determine the signals involved in the maintenance of T_{RM} in other tissues such as the gut and lung, which also persist in defined microenvironments (27, 28). In conclusion, our data demonstrate the dynamic nature of T_{RM} migration and persistence in skin and suggest a basis for the regulation of T-cell populations within an epidermal niche.

Materials and Methods

Mice. C57BL/6, gBT-I.EGFP, gBT-I.DsRed, gBT-I×B6.SJL-*PtprcaPep3b*/BoyJ (gBT-I.CD45.1), Lg-GFP, Lg.DTR-GFP (29), and CXCR6$^{GFP/+}$ mice were bred in the Department of Microbiology and Immunology, The University of Melbourne. AhR$^{-/-}$ were bred at The Babraham Institute. All mice were on a B6 background and were maintained under specific pathogen-free conditions. gBT-I (9) are T-cell receptor-transgenic mice recognizing the HSV-1 glycoprotein B-derived epitope $gB_{498–505}$. Animal experiments were approved by The University of Melbourne Animal Ethics Committee. Infection of mice was performed as described previously (3) and detailed in *SI Materials and Methods*.

Adoptive Transfers and Flow Cytometry. Adoptive transfers of 5×10^4 naïve gBT-I cells were performed intravenously. In vitro-generated gBT-I effector T cells were activated by peptide-pulsed splenocytes as described (4); $0.5–1 \times 10^6$ activated cells were transferred into recipients by intradermal injection (five 20-μL injections over a 1.5-cm^2 area of skin) using a 30-gauge needle. For DNFB treatment, 25 μL of 0.3% (vol/vol) DNFB in acetone/oil (4:1) were applied onto a 2-cm^2 area of skin. Three days after treatment, 5×10^6 in vitro effector gBT-I T cells were transferred into the mice. Cell isolation and antibodies used for flow cytometry are detailed in *SI Materials and Methods*.

Confocal and Two-Photon Microscopy. For immunofluorescence staining of fixed tissues, confocal microscopy and intravital two-photon microscopy, mice and tissues were prepared as described previously (3), as detailed in *SI Materials and Methods*. Images were acquired with Zeiss LSM700 or LSM710 NLO microscopes and processed using Imaris 7 software (Bitplane).

Quantitative RT-PCR. Mice containing 5×10^4 gBT-I CD8$^+$ T cells were infected with HSV and at various time points after infection gBTI T cells were FACS-sorted from skin and spleen using FACSAria III (BD). RNA extraction, cDNA synthesis, and preamplification was performed using the Taqman Gene Expression Cells-To-Ct Kit, Taqman PreAmp Master Mix, and assorted commercially available Taqman assays (all Life Technologies). Quantitative RT-PCR was performed with Taqman Fast Advanced Master Mix on a StepOnePlus Real-Time PCR cycler (both Life Technologies). The threshold cycle (Ct) of AhR for each cell population was normalized to the Ct of the Hprt housekeeping gene (ΔCt). Normalized AhR expression of each cell type was then compared with the normalized AhR expression of the naïve gBT-I population according to the $2^{(-\Delta\Delta CT)}$ method.

Simulating Cell Migration and Diffusion in the Skin. To determine the diffusion of motile T_{RM} within a rectangular strip of skin, the movement of cells was modeled by sampling with replacement from a dataset of observed displacements per minute of individually tracked in vivo cells. By the central limit theorem, and confirmed by numerical experiments, the distribution of the displacement of a cell over a period of t minutes was found to converge quickly to a Gaussian distribution for t much larger than 1. The movement of T_{RM} was modeled by a Wiener process appropriately fitted to the displacement data. A detailed description of the methods and calculations used can be found in *SI Materials and Methods*.

ACKNOWLEDGMENTS. We thank C. Jones, G. Davey, and M. Damtsis for technical assistance. This work was supported by the National Health and Medical Research Council of Australia and the Australian Research Council. M.V. is supported by a UK Biotechnology and Biological Sciences Research Council Institute Strategic Programme grant and European Research Council Grant 280307:Epithelial_Immunol.

1. Heath WR, Carbone FR (2013) The skin-resident and migratory immune system in steady state and memory: Innate lymphocytes, dendritic cells and T cells. *Nat Immunol* 14(10):978–985.
2. Mackay LK, et al. (2012) Long-lived epithelial immunity by tissue-resident memory T (TRM) cells in the absence of persisting local antigen presentation. *Proc Natl Acad Sci USA* 109(18):7037–7042.
3. Gebhardt T, et al. (2011) Different patterns of peripheral migration by memory CD4+ and CD8+ T cells. *Nature* 477(7363):216–219.
4. Gebhardt T, et al. (2009) Memory T cells in nonlymphoid tissue that provide enhanced local immunity during infection with herpes simplex virus. *Nat Immunol* 10(5):524–530.
5. Mueller SN, Gebhardt T, Carbone FR, Heath WR (2013) Memory T cell subsets, migration patterns, and tissue residence. *Annu Rev Immunol* 31:137–161.
6. Jiang X, et al. (2012) Skin infection generates non-migratory memory CD8+ T(RM) cells providing global skin immunity. *Nature* 483(7388):227–231.
7. Bromley SK, Yan S, Tomura M, Kanagawa O, Luster AD (2013) Recirculating memory T cells are a unique subset of CD4+ T cells with a distinct phenotype and migratory pattern. *J Immunol* 190(3):970–976.
8. van Lint A, et al. (2004) Herpes simplex virus-specific CD8+ T cells can clear established lytic infections from skin and nerves and can partially limit the early spread of virus after cutaneous inoculation. *J Immunol* 172(1):392–397.
9. Mueller SN, Heath W, McLain JD, Carbone FR, Jones CM (2002) Characterization of two TCR transgenic mouse lines specific for herpes simplex virus. *Immunol Cell Biol* 80(2):156–163.
10. Ariotti S, et al. (2012) Tissue-resident memory CD8+ T cells continuously patrol skin epithelia to quickly recognize local antigen. *Proc Natl Acad Sci USA* 109(48):19739–19744.
11. Chodaczek G, Papanna V, Zal MA, Zal T (2012) Body-barrier surveillance by epidermal γδ TCRs. *Nat Immunol* 13(3):272–282.
12. Igyártó BZ, Kaplan DH (2013) Antigen presentation by Langerhans cells. *Curr Opin Immunol* 25(1):115–119.
13. Strid J, Sobolev O, Zafirova B, Polic B, Hayday A (2011) The intraepithelial T cell response to NKG2D-ligands links lymphoid stress surveillance to atopy. *Science* 334(6060):1293–1297.
14. Jameson J, et al. (2002) A role for skin gammadelta T cells in wound repair. *Science* 296(5568):747–749.
15. Komori HK, et al. (2012) Cutting edge: Dendritic epidermal γδ T cell ligands are rapidly and locally expressed by keratinocytes following cutaneous wounding. *J Immunol* 188(7):2972–2976.
16. Toulon A, et al. (2009) A role for human skin-resident T cells in wound healing. *J Exp Med* 206(4):743–750.
17. Unutmaz D, et al. (2000) The primate lentiviral receptor Bonzo/STRL33 is coordinately regulated with CCR5 and its expression pattern is conserved between human and mouse. *J Immunol* 165(6):3284–3292.
18. Mackay LK, et al. (2013) The developmental pathway for CD103(+)CD8+ tissue-resident memory T cells of skin. *Nat Immunol* 14(12):1294–1301.
19. De Creus A, et al. (2002) Developmental and functional defects of thymic and epidermal V gamma 3 cells in IL-15-deficient and IFN regulatory factor-1-deficient mice. *J Immunol* 168(12):6486–6493.
20. Borkowski TA, Letterio JJ, Farr AG, Udey MC (1996) A role for endogenous transforming growth factor beta 1 in Langerhans cell biology: The skin of transforming growth factor beta 1 null mice is devoid of epidermal Langerhans cells. *J Exp Med* 184(6):2417–2422.
21. Schluns KS, Williams K, Ma A, Zheng XX, Lefrançois L (2002) Cutting edge: Requirement for IL-15 in the generation of primary and memory antigen-specific CD8 T cells. *J Immunol* 168(10):4827–4831.
22. Li Y, et al. (2011) Exogenous stimuli maintain intraepithelial lymphocytes via aryl hydrocarbon receptor activation. *Cell* 147(3):629–640.
23. Kadow S, et al. (2011) Aryl hydrocarbon receptor is critical for homeostasis of invariant gammadelta T cells in the murine epidermis. *J Immunol* 187(6):3104–3110.
24. Schenkel JM, Fraser KA, Vezys V, Masopust D (2013) Sensing and alarm function of resident memory CD8$^+$ T cells. *Nat Immunol* 14(5):509–513.
25. Puttur FK, et al. (2010) Herpes simplex virus infects skin gamma delta T cells before Langerhans cells and impedes migration of infected Langerhans cells by inducing apoptosis and blocking E-cadherin downregulation. *J Immunol* 185(1):477–487.
26. Gudjonsson JE, Johnston A, Dyson M, Valdimarsson H, Elder JT (2007) Mouse models of psoriasis. *J Invest Dermatol* 127(6):1292–1308.
27. Turner DL, et al. (2013) Lung niches for the generation and maintenance of tissue-resident memory T cells. *Mucosal Immunol*, 10.1038/mi.2013.67.
28. Anderson KG, et al. (2012) Cutting edge: Intravascular staining redefines lung CD8 T cell responses. *J Immunol* 189(6):2702–2706.
29. Kissenpfennig A, et al. (2005) Dynamics and function of Langerhans cells in vivo: Dermal dendritic cells colonize lymph node areas distinct from slower migrating Langerhans cells. *Immunity* 22(5):643–654.